# Supercritical $CO_2$ encapsulation of bioactive molecules in carboxylate based MOFs

Rebeca Monteagudo-Olivan,[a] María José Cocero,[b] Joaquín Coronas,[a,*] Soraya Rodríguez-Rojo[b,*].

[a] Chemical and Environmental Engineering Department, Instituto de Nanociencia de Aragón (INA) and Instituto de Ciencia de Materiales de Aragón (ICMA), Universidad de Zaragoza-CSIC, 50018 Zaragoza, Spain. Email: coronas@unizar.es.

[b] Bioeconomy Institute BioEcoUVa. High Pressure Process Group, Universidad de Valladolid, 47011 Valladolid, Spain. Email: soraya.rodriguez@uva.es.

## ABSTRACT

Caffeine and carvacrol were encapsulated using supercritical $CO_2$ (sc-$CO_2$) impregnation in MOFs, MIL-53(Al) and Mg-MOF-74, at different contact times. High additive loadings were achieved, 32.1 and 34.3% for caffeine, and for carvacrol 34.4 and 30.1%, respectively. The sc-$CO_2$ encapsulation was more effective compared to the typical liquid phase encapsulation in ethanol. In fact, the encapsulation in Mg-MOF-74 was only possible in sc-$CO_2$, null loading was observed in the liquid ethanol phase process. The products required no purification and the excess of additives could be reused. In all the studied cases, the materials maintained their crystalline structure and MIL-53(Al) displayed its characteristic flexibility adapting its structure to the additives. The total release of caffeine and carvacrol from Mg-MOF-74 was produced after 5 h in distilled water, while in the case of MIL-53(Al) no release was observed for 10 days.

## 1. INTRODUCTION

The potential applications of metal-organic frameworks (MOFs) are extensively studied due to their demonstrated high performance in different fields such as catalysis,[1] gas adsorption,[2] selective membranes[3] and drug-delivery,[4,5] among others. MOFs are highly porous materials which are made of metal centers connected by organic linkers, commonly dicarboxylates and imidazolates. Some of the most well-known MOFs are MOF-5,[6] MILs (Materials Institute Lavoisier)[7,8] and ZIFs (zeolitic imidazolate frameworks).[9] Encapsulation in MOF has been proposed for different applications, mainly for drug delivery in medicine and controlled release in cosmetics.[10–13] However, it also finds application for luminescence based sensors in which the adsorbed molecules enhance luminescence depending on the host-guest interactions,[14] heterogenization of homogeneous catalysts,[1] and medical imaging[15]. Regarding active compounds or drugs, MOFs show different sustained release from a few

hours to several days depending on the type of MOF and its stability in solution.[4] Among the MOFs studied for active molecules or drugs encapsulation, MIL-53(Fe) and MIL-53(Al) have been used in several reports,[4,16] while in vivo studies have been described for MIL-88A(Fe) and MIL-88B(Fe) modified with a polymer coating.[17] The encapsulation is normally carried out in liquid phase, after MOFs synthesis and processing, with generally good additive loadings.[18] In a previous work of the group the one-step encapsulation of caffeine in $NH_2$-MIL-88B(Fe) was reported, avoiding a multistep procedure, in which the synthesis and the encapsulation are carried out simultaneously.[19] Additionally, the encapsulation in MOF has been described by metal organic chemical vapor deposition (MOCVD) at high temperatures.[20]

The porosity of MOFs is not mostly accessible without an activation process, the excess of the organic linker and solvent has to be removed normally by successive washing with a specific solvent and thermal steps. In some MOFs, the thermal treatment may induce the partial collapse of their pores and the incomplete activation.[21,22] In order to overcome this handicap, several articles can be found on the use of supercritical-$CO_2$ (sc-$CO_2$) in a highly efficient activation and drying process of MOFs.[21,23] This supercritical technology has led to the largest BET specific surface areas ever reported, e.g. 7000 $m^2/g$ for Nu-110E.[24]

The supercritical conditions of $CO_2$ are relatively low, with a critical point at 301 K and 74 bar (NIST Database), and therefore easily achievable if they are compared with other compounds like water (647 K and 220 bar) or ethanol (514 K and 63 bar). In supercritical conditions, $CO_2$ displays an intermediate behavior between a liquid and a gas. It shows high diffusivity, as gases, which is useful to spread better into the microporosity of a given porous material. The density, comparable to liquids, allows its use as a relatively weak nonpolar solvent [25], that might have sufficient strength for various applications. Regarding encapsulation and precipitation, the literature about the use of supercritical fluids covers different types of carriers, e.g. polymers, biopolymers and aerogels.[26,27] As the sc-$CO_2$ operation leaves no residue, the use in food and medical/pharmaceutical industry has great interest to avoid undesirable contaminations.[25,26,28] Nevertheless, the applicability of sc-$CO_2$ is scarce in the encapsulation in porous inorganic or hybrid materials in powder form. To the best of our knowledge, only Matsuyama and co-workers applied the encapsulation with sc-$CO_2$ in MOFs, although in this case sc-$CO_2$ assisted the encapsulation and hexane as solvent was needed.[29] For zeolites, López-Periago and co-workers used sc-$CO_2$ as solvent to simultaneously synthesize and insert an active compound.[30]

From an industrial point of view, this process is advantageous because it is not necessary to manage water or organic solvents, and the waste is merely $CO_2$, which is naturally present in the atmosphere and eventually could be reused.[31] Additionally, the final product does not have to be purified because it is

in powder form as the starting material. Considering the case of poor soluble compounds in sc-$CO_2$, a co-solvent can be used to increase the solubility,[25,32] and then enhance the encapsulation process.

In this work, we have carried out the supercritical encapsulation of two additives, caffeine and carvacrol, into MOFs, MIL-53(Al) and Mg-MOF-74 (see Fig. 1). The former is a flexible hybrid net of 1D channels of terephthalate bidentate ligands connected by octahedral-coordinated $Al^{3+}$, interconnected by OH groups. The structure "breathes" or modifies the pore dimensions under different stimuli such as temperature or the presence of guest molecules, e.g. water.[7] In the hydrated material, known as MIL-53(Al) *lt*, water molecules are bound by hydrogen bonds that narrow the pore. Once the material is dried, named then MIL-53(Al) *ht*, the pores are opened.[7] This MOF shows high thermal stability to the extent that it can be activated by calcination at 380 °C.[7] Mg-MOF-74 is made of deprotonated 2,5-dihydroxyterephtelate and $Mg^{2+}$ which are coordinated to give rise a 12 Å honeycomb structure.[33] This MOF does not show flexibility, contains structural water molecules and presents a lower thermal stability.[33] Some MOFs can be degraded in aqueous media, and Mg-MOF-74 is sensitive to humidity.[34] This fact can be a handicap for several applications like gas separation or catalysis in presence of moisture. Nevertheless, it can be advantageous for controlled release and drug delivery, as reported for biopolymers and MOFs which are degraded leaving nontoxic residue.[25,35–37] Once MIL-53(Al) and Mg-MOF-74 were degraded, the inorganic and the organic parts would be obtained separately. The inorganic part corresponds to ions of aluminum and magnesium, both present in normal diets. Furthermore, the former is present in drugs such as almagate (Almax™), which is used as anti-acid, and the latter is used as dietary supplement. The organic rests are terephthalate and 2,5-dihydroxiterephthelate which could be potentially biocompatible like for other similar ligands.[15,38]

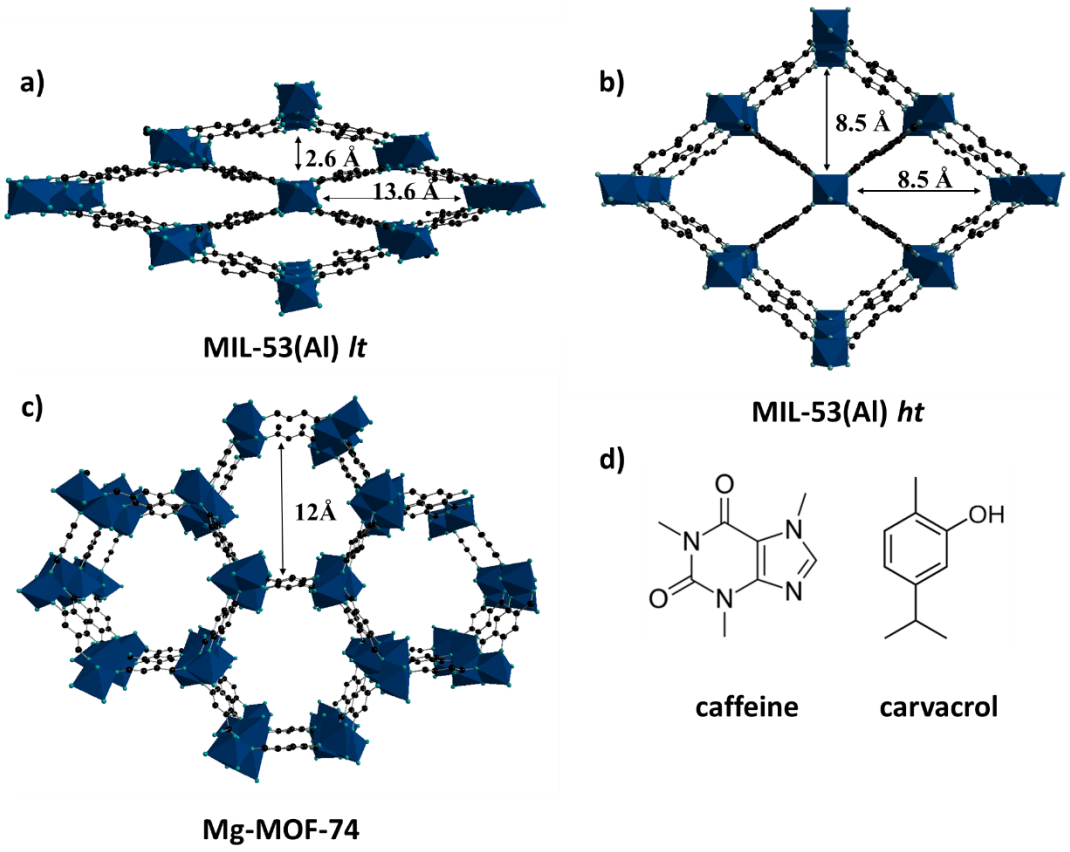


**Figure 1.** MOF guest structures used in this work with channels sizes, MIL-53(Al) (a and b) and Mg-MOF-74 (c). Atomic color code: carbon (black), oxygen (light blue) and metal coordination (dark blue). These structures were made with Diamond 3.2. using the corresponding CIF files.[7,33] The molecular structures of the studied guest additives (d).

The pure additive compounds tested for this work are caffeine and carvacrol (see Fig. 1d), both of them show relatively high solubility in sc-$CO_2$. In fact, caffeine is commonly used as additive and is broadly studied in supercritical fluids.[39,40] Decaffeination of coffee is mass produced by extraction with sc-$CO_2$ in substitution of toxic and pollutant dichloromethane.[41] Caffeine is commonly used as model drug or additive for demonstration of novel encapsulation procedures, e.g. in MOFs[18,19,42], silica[43], and polymers.[44] Even though encapsulation find major applications for non hidrosoluble or sensitive compounds, the encapsulation and release of hydrosoluble caffeine has been reported useful in textiles for cosmetic applications[44,45] or for oral administration with chewing gum *versus* capsules.[46] Carvacrol is also a natural occurring compound, one of the main components of oregano essential oil. It has been studied with supercritical fluids and its solubility has been reported at different conditions.[47] Carvacrol shows antimicrobial properties[48,49] and has been previously encapsulated

in different matrices such as starch,[27] milk protein[50] and chitosan.[51] Carvacrol has been studied as additive for food preservation in packaging materials[52] and biofilms[53] with controlled release.

Herein we achieved the encapsulation in pure supercritical $CO_2$ phase of soluble additives, caffeine and carvacrol, in carboxylate based MOFs, MIL-53(Al) and Mg-MOF-74. This process required no purification and produced no waste. We compared the results of the sc-$CO_2$ impregnation with those achieved in liquid impregnation to highlight the benefits of the proposed process. Additionally, the effects of the encapsulation on the materials were characterized by X-ray diffraction (XRD) to check the crystalline structure stability after processing the starting materials and the potential changes in the flexible structure of MIL-53(Al).[7,8] We analyzed the samples by Raman spectroscopy to study the additive-MOF interactions; this technique has been widely used for host-guest systems[54–57] to gather information about the configuration of the guest additive in the host MOF. Finally, as a proof of concept of the potential use for controlled release, the additive release of the sc-$CO_2$ impregnated samples was monitored through time.

## 2. EXPERIMENTAL

### 2.1-Materials

For MOF synthesis the reactants were aluminum nitrate nonahydrate ($Al(NO_3)_3 \cdot 9H_2O$, Sigma Aldrich, ≥98%), magnesium hydroxide ($Mg(OH)_2$, Alfa Aesar, 95-100 %), terephthalic acid ($H_2BDC$, Sigma Aldrich, 98%) and 2,5-dihydroxyterephthalic acid (6 mmol, $H_4DOBDC$, TCI, >98%). The synthesis solvents were distilled water and tetrahydrofuran (THF, Scharlab, >98%). Methanol (MeOH, Scharlab, >99%) was used for washing. Additives were carvacrol (150 g/mol, Sigma Aldrich, 99% FG) and caffeine (194 g/mol, Sigma Aldrich, 99%). For supercritical $CO_2$ encapsulation (Carburos Metálicos S.A., 99.95%) and for liquid encapsulation absolute ethanol were used. Analysis solvents for CG-MS were MeOH (Scharlab, analysis grade) and acetone (PanReac, analysis grade). Analysis solvents for HPLC were Milli-Q water (Millipore), phosphoric acid (Acros Organic, aqueous solution 85%), MeOH (Scharlab, analysis grade) and acetonitrile (Scharlab, analysis grade). All the chemicals were used as received.

### 2.2- Synthesis of MOFs

**Synthesis of MIL-53(Al), Al(OH)BDC.** From a previous report,[7] 15.6 g of $Al(NO_3)_3 \cdot 9H_2O$ (41.7 mmol) and 3.36 g of $H_2BDC$ (20.1 mmol) were added to a 400 mL Teflon-lined stainless steel autoclave (Berghof DAB-3) where 250 mL of distilled water was poured to form a white dispersion. The system

was sealed and placed in an oven for 3 days at 220 °C. The product was recovered by centrifugation at 10,000 rpm for 10 min (Allegra® X-15R Centrifuge), washed with distilled water and recovered also by centrifugation at the same conditions. The white product was dried at room temperature overnight and activated by calcination for 24 h at 380 °C (see Fig S1). Yield with respect to $H_2$BDC: 61%

**Synthesis of Mg-MOF-74, [$Mg_2$(DOBDC)($H_2O$)$_2$]· 8$H_2O$.** From the original synthesis,[33] including some small variations, 1.188 g of $H_4$DOBDC (6 mmol) was dissolved in 120 mL of THF in a glass flask. Then a solution of 0.699 g of $Mg(OH)_2$ (12 mmol) in 40 mL of distilled water was added and the mixture was heated at 80 °C for 5 h under reflux. A yellow solid was recovered by centrifugation at 10,000 rpm for 10 min and washed several times with MeOH with an ultrasound treatment for 2 min between washings. The yellow product was dried at room temperature overnight (see Fig S1). Yield with respect to $H_4$DOBDC: 79%.

### 2.3- Supercritical $CO_2$ and liquid impregnation

**Supercritical $CO_2$ impregnation.** The experimental set-up used to prepare encapsulated additive@MOFs (i.e. carvacrol@MOF and caffeine@MOF) is shown in Fig. 2. The stored $CO_2$ (1) is carried to a cooler in order to assure liquid state (2) and pumped (3) to reach a pressure of 100 bar inside the vessel (4). Liquid carvacrol or solid caffeine was placed at the bottom of the stainless steel vessel (4) and the MOF was separated above by a metallic mesh to avoid direct contact. The vessel was put in an oven (5) which was connected to a temperature sensor inside the recipient (4). The selected temperature was 40 °C, a little above the supercritical conditions, but not a very high value because it was intended to have soft conditions of temperature so that this methodology can be extended to temperature sensitive molecules like carvacrol, and additionally, in this manner, the potential large scale costs are also reduced. As mentioned above, both compounds exhibit high solubility in sc-$CO_2$. The temperature and pressure were selected to achieve a high value of solubility of both additives, and the amount of additive was chosen above the saturation concentration in the described conditions. The volume of the recipient was 85 $cm^3$ and the density of sc-$CO_2$ in the working conditions was 0.686 g/mL (NIST database). The solubility, in molar fraction, of caffeine and carvacrol in sc-$CO_2$ at 40 °C and 100 bar is reported to be $6.3 \cdot 10^{-5}$[39,40] and 0.02[47], respectively. To have a large excess, 1.00 g caffeine and 5.00 mL carvacrol were used in the respective experiments. To ensure the solubilization of the additive in the $CO_2$, the cell was provided with a magnetic mixer. After the predefined contact time, the cell was depressurized through a micrometric valve with a velocity of depressurization of 20 bar/min. To avoid freezing, a heater was placed in the exit pipe (6). After the experiments, the excess of additive could be re-used as it was not damaged during the process.

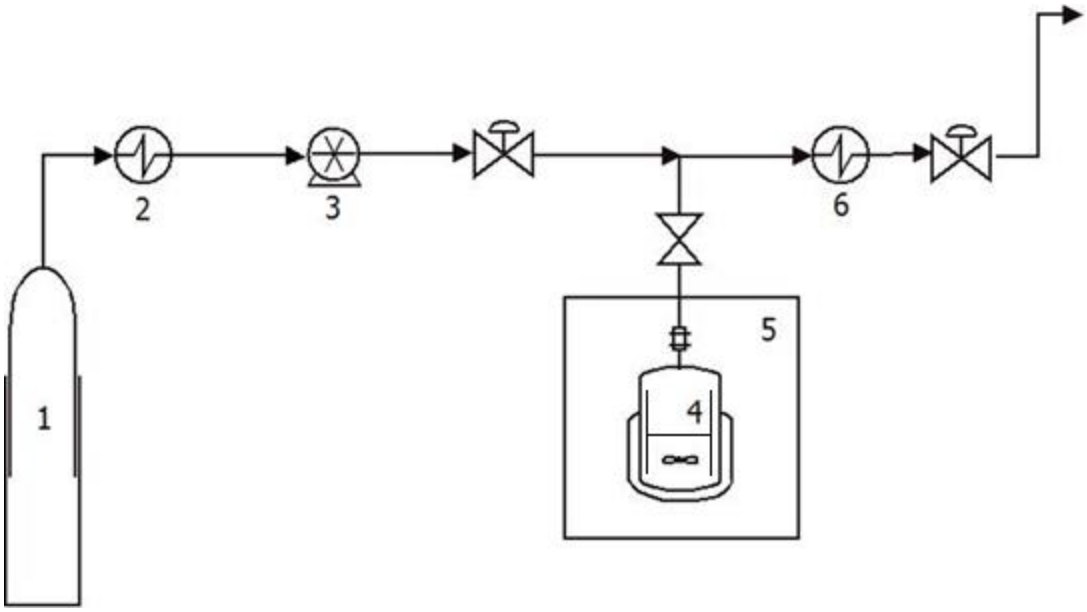


**Figure 2.** Schematic set-up for sc-$CO_2$ encapsulation: (1) $CO_2$ cylinder, (2) cooler, (3) pump, (4) encapsulation vessel, (5) oven, (6) Heater.

**Liquid ethanol impregnation.** In a vial, 100 mg of MOF, MIL-53(Al) or Mg-MOF-74, was suspended in a concentrated solution (10 mL) of caffeine (4 g/L) or carvacrol (50 g/L). The use of ethanol as medium was selected considering the low stability of Mg-MOF-74 in water and the better solubility of the additives in this alcohol. At room temperature the samples are impregnated with magnetic stirring. After 14 h, the solids were recovered by centrifugation at 10,000 rpm for 10 min and dried at room temperature overnight.

### 2.4- Controlled release

The releases of caffeine and carvacrol from MIL-53(Al) and Mg-MOF-74 were monitored as a function of time. The selected samples were those with the highest obtained loadings with sc-$CO_2$, i.e. caffeine@MIL-53(Al) and caffeine@Mg-MOF-74, both samples impregnated for 24 h, and carvacrol@MIL-53(Al) and carvacrol@Mg-MOF-74 impregnated for 14 h. The loaded material (additive@MOF, 20 mg) was suspended in a beaker with 0.5 L of distilled water, to ensure sink conditions, with magnetic stirring bar at 25 °C. At each selected time an aliquot of 1.2 mL was collected, and the same volume was replaced with water. The sample was centrifuged for 2 min at 5,000 rpm (Microfuge 16, Beckman Coulter) and the supernatant was filtered (PTFE, 0.22 μm) for HPLC analysis.

### 2.5- Characterization

### 2.5.1- Determination of caffeine and carvacrol loadings

**Extraction and gas chromatography-mass spectroscopy (CG-MS).** The extraction was carried out with 10.0 mg of additive@MOF in 1.5 mL of acetone for caffeine and 1.5 mL of ethanol for carvacrol containing samples. Each suspension was sonicated for 0.5 h and the liquid was separated from the solid by centrifugation at 5,000 rpm for 5 min. The solution of the extracted additive was filtered previously to the analysis with 0.22 μm filters. The concentrations were determined by CG-MS (7890C GC/5977A MSD Agilent Technologies) equipped with a HP-5MS capillary column (30 m x 0.25 mm x film thickness 0.25 μm). The carrier gas was helium at a flow rate of 0.7 mL/min with 1 μL of injection volume and a 300:1 split ratio. The injection was carried out with the column oven at 105 °C, then heated to 220 °C (4 °C/min) and to 250 °C (15 °C/min). MSD transfer line temperature was 250 °C. The electron ionization system for detection operated at an ionization voltage of 70 eV. The calibration ranges for caffeine and carvacrol were, respectively, 0.5-1.5 mg/mL and 1.0-4.0 mg/mL. Samples analyses were performed in duplicate and the corresponding standard deviations were calculated. The loading values were calculated as (g additive/g dry MOF)·100 and dry MOF was determined by thermogravimetry (see below).

**2.5.2- Pore occupation: $N_2$ and $CO_2$ adsorption.** The $N_2$ adsorption capacity of MIL-53(Al) and additive@MIL-53(Al) was analyzed at 77 K with a TRIStar 3000 instrument and specific surface area was calculated by BET method. The $CO_2$ isotherms and uptakes at 273.15 K of Mg-MOF-74 and additive@Mg-MOF-74 were obtained with a Micrometrics ASAP 2020 instrument. Previously to analysis, outgassing was carried out under vacuum for 5 h at 150 °C.

**2.5.3- X-ray diffraction (XRD) of crystalline materials**. The MOF and additive@MOF samples were characterized by XRD to check the effects in crystallinity before and after the sc-$CO_2$ and common liquid phase encapsulations. The measurements were recorded in a Siemens D-5000 diffractometer (45 kV, 40 mA) with a copper anode with a graphite monochromator in $CuK_{\alpha 1}$ radiation ($\lambda$=1.540 Å) in the 4-40° 2θ range and a scanning rate of 0.03°/s.

**2.5.4- Raman spectroscopy.** The host-guest interactions between the additive and the MOF were studied by Raman spectroscopy (WITec alpha 300) with the 783 nm laser and working at 17 mW. The integration time for each measurement was 1.5 s and the data recording were taken with 25 accumulations and a resolution of 2 $cm^{-1}$.

**2.5.5-Thermogravimetric analysis (TGA).** Using a Mettler Toledo TGA/SDTA 851e instrument, the TGA analyses of the samples were carried out in 70 μL alumina pans and heated up under air atmosphere to 700 °C with a ramp of 10 °C/min.

**2.5.6- Particle morphology and scanning electron microscopy (SEM).** The powder materials, before and after the encapsulation processes, were studied by SEM (Inspect F50) coated previously with a thin film of platinum to ensure the conductivity of samples.

**2.5.7-Monitoring caffeine and carvacrol release by high performance liquid chromatography (HPLC).** The concentrations of additives during the release experiments were analyzed by HPLC, in a Waters 1515 system equipped with a C18 column (SunFire 4.6 x 250 mm, 5 μm) and coupled with a UV-Vis dual λ absorbance detector (Waters 2487), operating in isocratic mode at 40 °C with a mobile phase flow of 2 mL/min. The mobile phase for caffeine was composed by 75% of phosphate buffer 0.025 M in Milli-Q water at pH 3 and 25% of MeOH, meanwhile for carvacrol determination it was composed of 50% acetonitrile and 50% Milli-Q water. Calibration ranges for caffeine and carvacrol were for both 2.0-10.0 mg/L. Sample analyses were performed in duplicate and the corresponding standard deviations were calculated.

## 3. RESULTS AND DISCUSSION

### 3.1- Effect of contact time

Fig. 3 shows the effect of contact time in the sc-$CO_2$ encapsulation of caffeine and carvacrol in MIL-53(Al) and Mg-MOF-74 in the conditions described above. For caffeine@MIL-53(Al) (see Fig. 3a) a gradual increase was observed until 24 h when the loading reached a value of 32.1%. In opposition, the sc-$CO_2$ encapsulation of caffeine in Mg-MOF-74 showed a remarkable difference between 4 and 14 h, from 3.2% to 17.7%. This difference was not observed in MIL-53(Al), which shows a more gradual loading increase. It could be explained by the high content of water present in Mg-MOF-74 (see the ca. 38% weight loss below 150 °C in Fig. 4c) and by the structural role of part of it as described by Dietzel *et al.* 2008[33]. This water cannot be thermally evacuated during pore activation (removing molecules inside the pores) without inducing the structure collapse.[33] It might create some transport resistance against the diffusion of sc-$CO_2$ and caffeine into the pores; therefore, the encapsulation kinetics was slower in this case. The low solubility of water in $CO_2$[58,59] can contribute to the resistance of the withdrawal of water from the MOF (to release its porosity for the guest) and consequently the loading is hindered at short processing times. After the removal of some water by sc-$CO_2$ (Fig 4c), high caffeine loadings were achieved after 24 h (34.3%) in Mg-MOF-74.

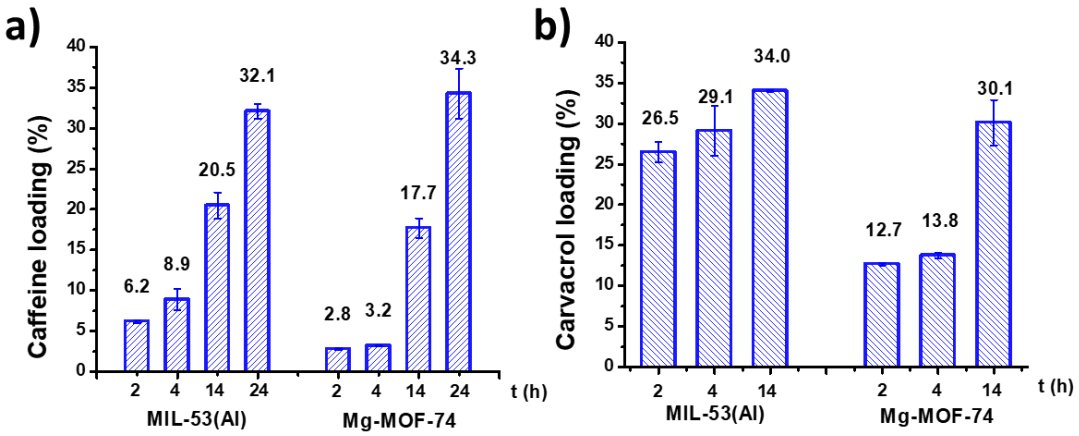


**Figure 3.** Effect of contact time in sc-$CO_2$ encapsulation at 40 °C and 100 bar in MIL-53(Al) and Mg-MOF-74 for caffeine (a) and carvacrol (b).

A fast encapsulation of carvacrol in MIL-53(Al) was observed after 2 h of contact time with a loading value of 26.5% (Fig. 3b). If the contact time was increased to 14 h the loading achieved was 34.0%. The relatively high solubility of carvacrol in the working conditions (40 °C and 100 bar, see section 2.3) and its size, smaller than that of caffeine, favored a more efficient and faster loading. Carvacrol was considered a smaller molecule than caffeine in agreement with their respective molar masses of 150 g/mol and 194 g/mol and the bulkier molecular structure of the latter (see Fig. 1). In the case of the encapsulation of carvacrol in Mg-MOF-74, the same kinetic effect was observed, the loading increase was more remarkable between 4 and 14 h than in the 2-4 h interval.

Fig. 4c shows the thermal step removal of caffeine in Mg-MOF-74 corresponding to the sc-$CO_2$ encapsulation at 14 h and the reduced amount of water with respect to the starting material. Therefore, it seems that the encapsulation is concomitant with a partial substitution of the water by the additive. On the contrary, the loading of caffeine in MIL-53(Al) was directly produced, considering that the presence of water in the starting material was significantly lower (3%, see Fig. 4). Noticeably, in the curve for carvacrol@Mg-MOF-74 impregnated with sc-$CO_2$, the removal steps of water and carvacrol are consecutives and a single step is observed in the corresponding TGA curve.

After the encapsulation the pore occupation was verified by the decrease in the capacities of MIL-53(Al) to adsorb $N_2$ and of Mg-MOF-74 to adsorb $CO_2$ (Table 1 and Fig. S2). The previous outgassing was carried out at 150 °C in all cases, thus the additives were not removed during this step. Consequently, the BET specific surface area for MIL-53(Al) was low (761 $m^2/g$), while if degasification was carried out at 200 °C it increased to 1100 $m^2/g$, in agreement with the reported value of 1140 $m^2/g$.[7] The impregnated MIL-53(Al) samples show almost null BET area, which is in agreement with high encapsulations of caffeine and carvacrol in the MOF pores. Analogous results were found in terms of $CO_2$ adsorp-

tion capacities (see Table 1) of caffeine@Mg-MOF-74 (1.4 mmol/g) and carvacrol@Mg-MOF-74 (0.4 mmol/g), compared to that of Mg-MOF-74 (12.0 mmol/g), similar to the reported value ca. 10.7 mmol/g.[60] These lower $CO_2$ adsorption capacities agree with the Mg-MOF-74 porosity occupied by the additive molecules. Nevertheless, the retained $CO_2$ adsorption capacity suggests that not all the porosity was occupied by the additives because of the rigid structure of this MOF and the water structural molecules, which do not allow a facilitated diffusion through the pores.

Table 1. Adsorption before and after the sc-$CO_2$ encapsulation with a contact time of 14 h at 100 bar and 40 °C. BET specific surface areas of MIL-53(Al) and impregnated samples (left) and $CO_2$ adsorption capacities at 0 °C and 1 atm of Mg-MOF-74 and impregnated samples (right).

| | $S_{BET}$ ($m^2$/g) | | $CO_2$ uptake (mmol/g) |
|---|---|---|---|
| MIL-53(Al) | 761 | Mg-MOF-74 | 12.0 |
| caffeine@ MIL-53(Al) | 7 | caffeine@ Mg-MOf-74 | 1.4 |
| carvacrol@ MIL-53(Al) | 5 | carvacrol@ Mg-MOF-74 | 0.4 |

### 3.2- Comparison of sc-$CO_2$ versus liquid ethanol phase encapsulations

Fig. 5 compares the sc-$CO_2$ encapsulation with the traditional liquid phase (using ethanol which shows good solubility for caffeine and carvacrol) after 14 h of contact time in both cases. In general, the loading values were higher for supercritical encapsulation, even if in case of MIL-53(Al), the difference was not very substantial for caffeine. However, only a 6% of carvacrol loading was achieved in liquid phase *vs* a 34.0% in sc-$CO_2$. The loading of caffeine in MIL-53(Al) in liquid phase of ethanol (16.4%) was significantly higher than that of carvacrol (6.3%), meanwhile the behavior was reversed in supercritical conditions and less caffeine (20.5%) was loaded than carvacrol (34.0%).

For Mg-MOF-74 the differences were more noticeable between sc-$CO_2$ and ethanol. In fact, the encapsulation in liquid phase was not achieved in Mg-MOF-74 with none of the additives. In agreement with this, the corresponding TGA curves also show the differences among these samples (see Fig. 4). In the liquid phase encapsulation, the resulting materials have almost identical curves to the starting Mg-MOF-74. Meanwhile, the samples with sc-$CO_2$ show the removal step of caffeine and an increased amount of the organic part for carvacrol at a temperature similar to that corresponding to the removal of structural water. For MIL-53(Al) the TGA curves suggest that some non-desired ethanol solvent would remain in the pores of the material after the liquid encapsulation of caffeine (Fig 4a) and the subsequent drying at room temperature.

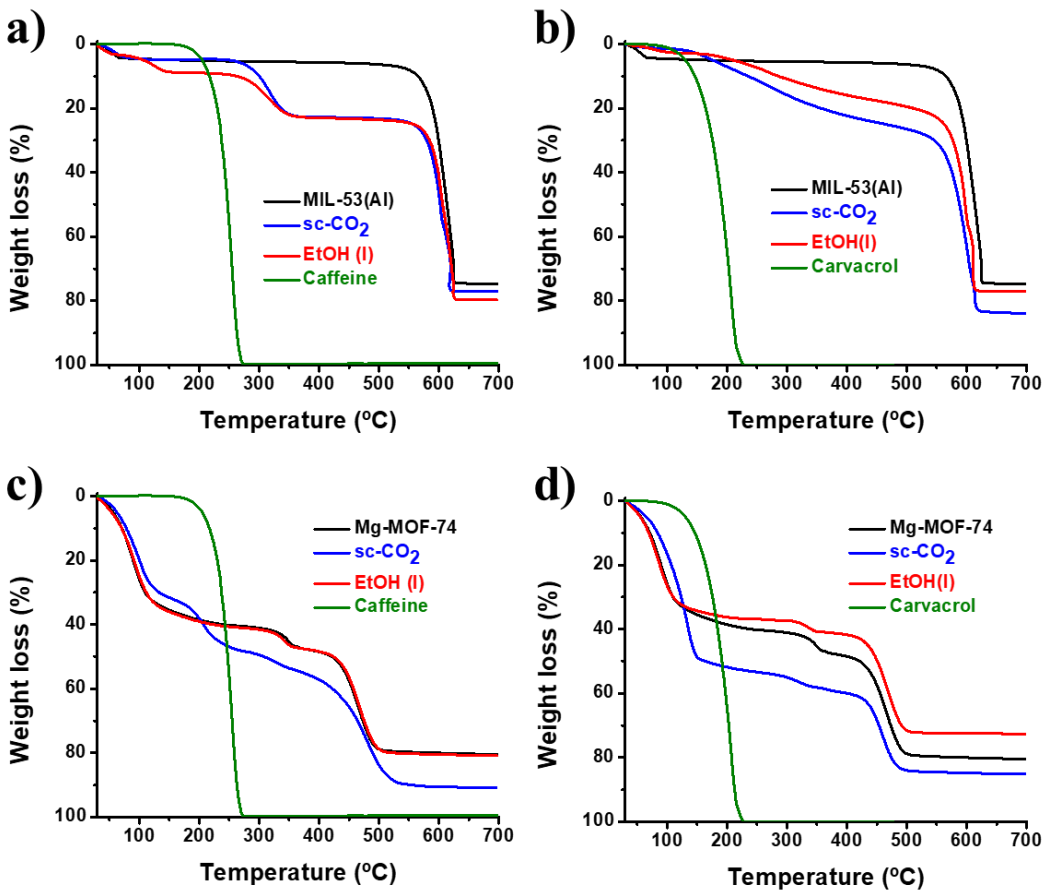


**Figure 4.** TGA curves of sc-$CO_2$ encapsulations at 40 °C and 100 bar and ethanol liquid encapsulations at 25ºC in MIL-53 of caffeine (a) and carvacrol (b), and in Mg-MOF-74 of caffeine (c) and carvacrol (d). The encapsulation contact time was 14 h in all the experiments.

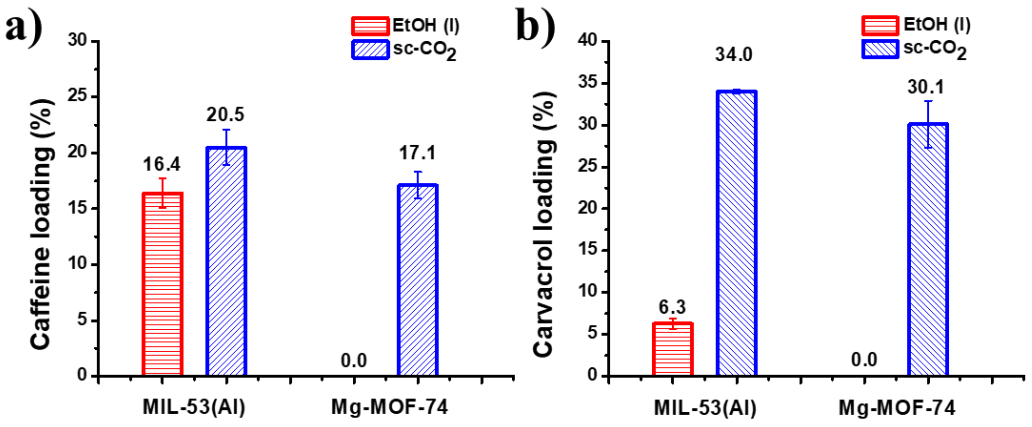


**Figure 5.** Compared encapsulation values of caffeine (a) and carvacrol (b) in MIL-53(Al) and Mg-MOF-74 with sc-$CO_2$ encapsulation versus ethanol liquid phase encapsulation at 25 °C for a contact time of 14 h.

Finally, Figs. S3 and S4 depict SEM images of MIL-53(Al) and Mg-MOF-74, respectively, before and after encapsulations. As reported elsewhere,[7,33] the former displays a polyhedral morphology, while in the later the particles are needle-like. These shapes were maintained after both types of encapsulations in the described conditions.

### 3.3- Structural Characterization: XRD and Raman spectroscopy studies

The MOF crystalline structure was studied by XRD before and after sc-$CO_2$ and liquid ethanol phase encapsulations. The interpretations were correlated with the flexible structure for MIL-53(Al)[7] and the rigidity of Mg-MOF-74.[33] The water molecules of the MIL-53(Al) pores create hydrogen bonds between the carboxylates of the terephthalate ligands that narrow the pores, giving rise to the so-called *lt* form, after calcination the pores open producing the *ht* form.[7] The caffeine@MIL-53(Al) pattern obtained by sc-$CO_2$ treatment seems to arise from a combination of *ht* and *lt* configurations (Fig. 6Ab). The *lt* peaks (Fig. 6Aa) are kept with lower intensity although the main peak in the *ht* form (Fig. 6Ae) appears clearly. The size of caffeine is considerable, therefore its diffusion through the MOF pores may be hindered and with different potential configurations. Other additional peaks present in the XRD pattern suggest a mixture of the two MIL-53(Al) pore structures adapted to the guest caffeine molecule. The peaks of caffeine are not observed, consistent with the absence of external caffeine.[61] The XRD pattern corresponding to the liquid encapsulation in Fig. 6Ac seems undefined, suggesting the presence of retained solvent. Fig. 6B shows the different patterns corresponding to carvacrol@MIL-53(Al). The liquid and supercritical encapsulations arose with similar patterns between them (Figs. 6Bb and 6Bc) and with some common peaks of the pattern of MIL-53(Al) *ht*, implying the pore opening in both and the removal of the hydrogen bonding water, in agreement with the absence of water in the TGA curves (Fig. 4b).

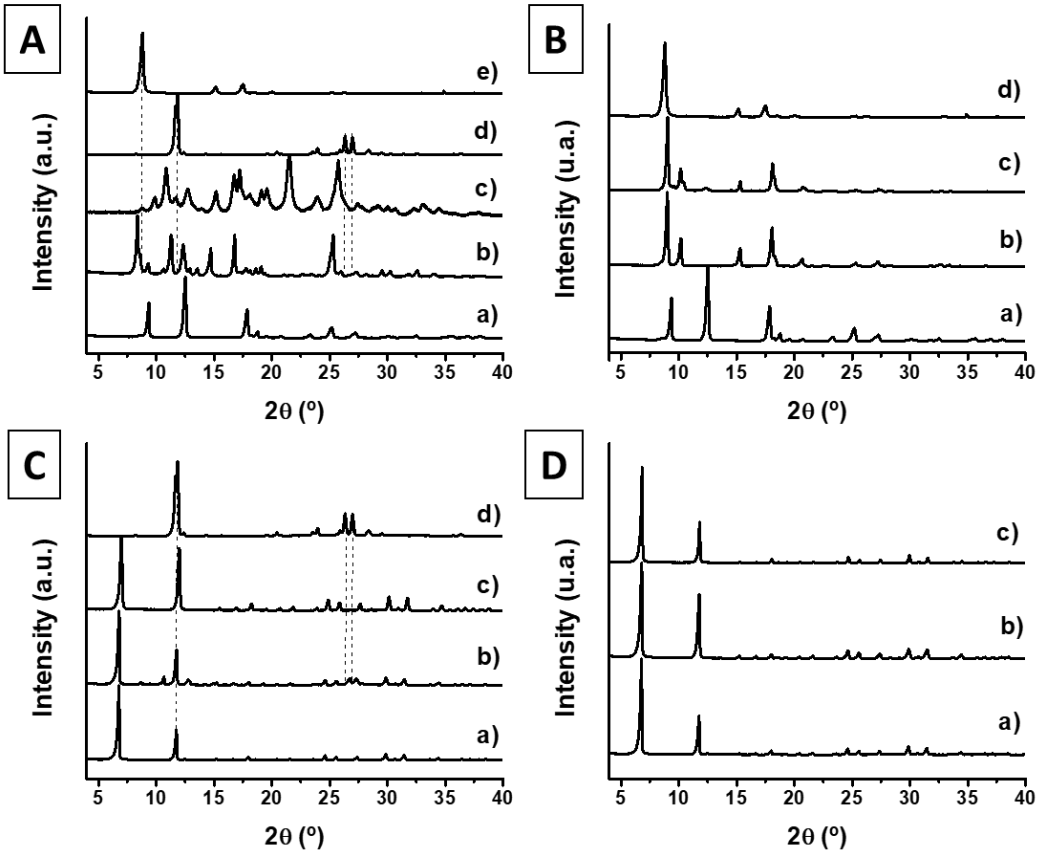


**Figure 6.** XRD patterns of (A) MIL-53(Al) *lt* (a), caffeine sc-$CO_2$ encapsulation (b), caffeine liquid phase encapsulation (c), caffeine (d) and MIL-53(Al) *ht* (e); (B) MIL-53(Al) *lt* (a), carvacrol sc-$CO_2$ encapsulation (b), carvacrol liquid phase encapsulation (c), and MIL-53(Al) *ht*; (C) Mg-MOF-74 (a), caffeine sc-$CO_2$ encapsulation (b), caffeine liquid phase encapsulation (c) and caffeine (d); and (D) Mg-MOF-74 (a), carvacrol sc-$CO_2$ encapsulation (b) and carvacrol liquid phase encapsulation (c). The encapsulation contact time was 14 h in all the experiments.

For the encapsulations in Mg-MOF-74, the XRD patterns are similar to that of the starting Mg-MOF-74 (see Figs. 6C and 6D). These data imply that none of the encapsulation processes affected the bulk crystallinity of the rigid structure.

The host-guest interactions were studied by Raman spectroscopy which provides information about the structure of the samples and the molecular interactions. The nature of the material structure has influence on the interpretation of the Raman results shown in Fig. 7 and Tables S1-S4. The encapsulations of caffeine in MIL-53(Al) show similar Raman shifts corresponding to the terephthalate bands of the MOF, although the relative intensity is remarkably changed for sc-$CO_2$ encapsulation (see Fig. 7A and Table S1) with respect to the starting material or to that achieved by liquid phase encapsulation for bands at 867, 1469 and 1612 $cm^{-1}$ which corresponds to the deformation of aromatic C-H, symmetric stretching of $CO_2^-$ and ring C=C stretching. The modification of the intensities in case of supercritical

encapsulation may be attributed to the modification of the polarization of terephthalate intramolecular bonds in the MIL-53(Al) structure and to the more effective pore occupation by caffeine (See Fig. 4). The molecule of caffeine can be placed in parallel with the ligand terephthalate and hence the heteroatoms of caffeine induce the polarizability of C-H bonds of the ligand increasing the Raman intensity (in Raman spectroscopy the intensity is related with the polarizability of the vibrational mode). Interestingly, this fact induces the contrary effect on the stretching of C=C of the aromatic ring. The opening of the MIL-53(Al) pore (observed by XRD, see Fig. 6A) had to remove the hydrogen bonding in the *lt* form between two adjacent carboxylates and can be the cause of the reduced intensity of one of the modes of the carboxylate. The hydrogen bonding may be partially present considering that there is some water after the supercritical encapsulation (see TGA curves in Fig 4a) and that the XRD is altered (with respect to the pristine MOF) which arises from different pore fillings or configurations (see Fig 6A). As opposed, the Raman spectrum of the sample caffeine@MIL-53(Al) obtained in liquid phase encapsulation shows almost no changes with respect to the starting material which indicates the weaker interactions with pore walls.

Fig. 7B shows the Raman spectra for carvacrol@MIL-53(Al) encapsulations (see also Table S2). The most important differences are in the stretching modes of the MOF carboxylates for both processes. In agreement with TGA and XRD, in which the open structure of the *ht* form is observed, no water, displaced by carvacrol, is present in the MOF porosity. The shifts of the $CO_2^-$ stretching (*st*) bands can be caused by the breaking of the water-MOF hydrogen bond and its potential substitution by hydrogen bonds between the aromatic alcohol of carvacrol and the MOF. The more acidic character of the phenol in carvacrol favors its actuation as hydrogen donor which it is not present with the saturated molecule of ethanol (media for liquid encapsulation). Therefore, in both liquid and sc-$CO_2$ phases, the Raman spectroscopy suggests that hydrogen bond interactions carvacrol-MIL-53(Al) influenced the encapsulation. Another noticeable difference is the single new band at 187 $cm^{-1}$ for both encapsulations which is assigned to lattice vibrations of the expansion and contraction of MIL-53(Al) *ht* flexible network (this fact reminds to the radial breathing mode of carbon nanotubes).[62] In this region of the spectrum, there are several very weak bands in the *lt* form and in the caffeine encapsulation a band appears with higher intensity than others but the pore is not totally open, as it is observed in the diffraction pattern.

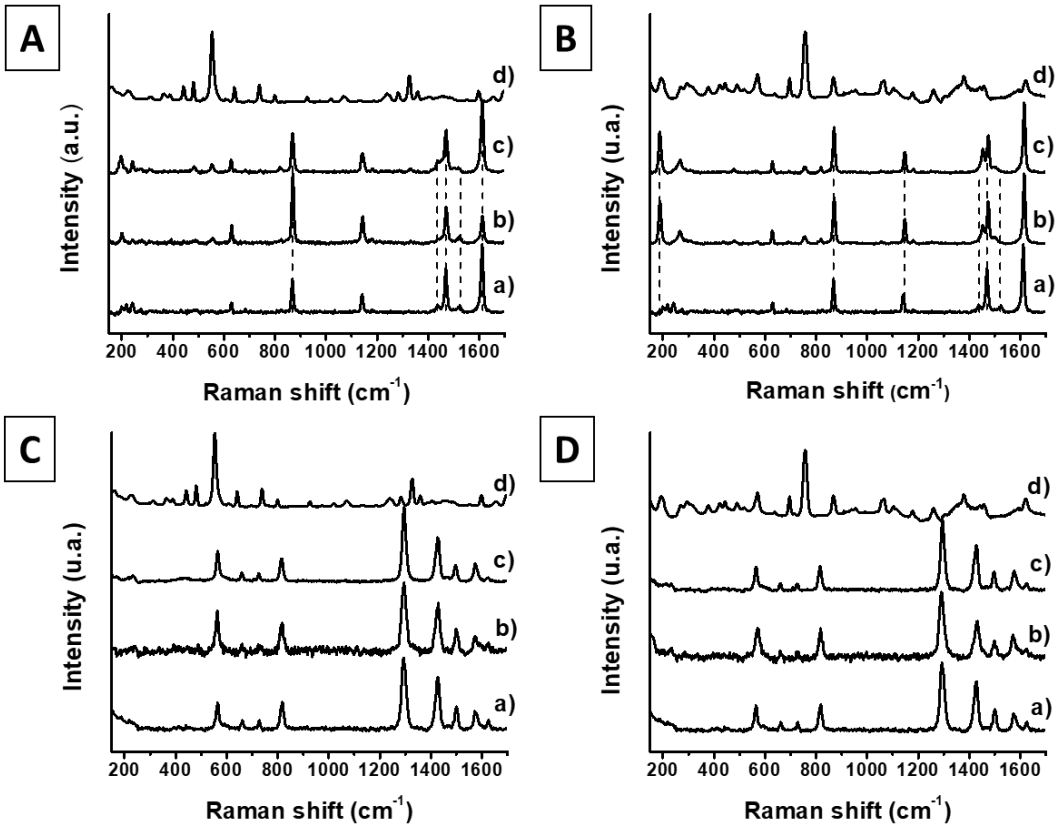


**Figure 7.** Raman spectra of (A) MIL-53(Al) *lt* (a), caffeine sc-$CO_2$ encapsulation (b), caffeine liquid phase encapsulation (c) and caffeine (d), (B) MIL-53(Al) *lt* (a), carvacrol sc-$CO_2$ encapsulation (b), carvacrol liquid phase encapsulation (c) and carvacrol (d), (C) Mg-MOF-74 (a), caffeine sc-$CO_2$ encapsulation (b), caffeine liquid phase encapsulation (c) and caffeine (d), (D) Mg-MOF-74 (a), carvacrol sc-$CO_2$ encapsulation (b), carvacrol liquid phase encapsulation (c) and carvacrol (d). The encapsulation contact time was 14 h in all the experiments.

In opposition, the Raman spectra of the encapsulations in Mg-MOF-74 show no remarkable shifting neither for caffeine nor carvacrol (see Fig. 7C-D and Tables S3-S4). This fact was expected for the liquid phase encapsulation considering that the loading of additives was null (or, in any case, perhaps some water could have been replaced by ethanol). Alternatively, the spectra of the encapsulation in sc-$CO_2$ show more background noise for both additives, caffeine and carvacrol, which could be due to the increase of unspecific interactions. In the pure MOF the pores are filled with water (around 35% in weight, see the TGA in Fig. 4) which was not totally removed after the encapsulation (around 25%) for caffeine@Mg-MOF-74, neither for carvacrol@Mg-MOF-74, in which the remaining water cannot be estimated from the TGA curve because the removal step of water is consecutive to that of carvacrol. This presence of water could lead to reduced additive-MOF interactions. Additionally, the structure of Mg-MOF-74 is rigid and less changes can be expected in comparison with MIL-53(Al). The increased

noise can also be assigned to punctual crystal damage although the bulk crystallinity of Mg-MOF-74 seems unaltered (see Figs. 6C-D).

### 3.4- Controlled release

The release of caffeine and carvacrol in aqueous media was studied at room temperature for the highest loaded samples in sc-$CO_2$ (24 h for caffeine@MOF and 14 h for carvacrol@MOF). Two different behaviors were observed for additive@Mg-MOF-74 and additive@MIL-53(Al). In distilled water the former releases most of the impregnated caffeine and carvacrol in 5 h (see Fig. 8a) due to the simultaneous hydrolysis of Mg-MOF-74.[63] However, the two additive@MIL-53(Al) materials showed no release for 10 days. The suspended material in the release media was recovered by centrifugation after that time and analyzed by thermogravimetry to evidence the presence of caffeine and carvacrol remained in the corresponding two additive@MIL-53(Al) materials (see Fig. 8b). The compared curves with the starting materials shows a small decrease of both additives in MIL-53(Al) that was not evidenced during the release experiments or the amount was below the limit of quantification.

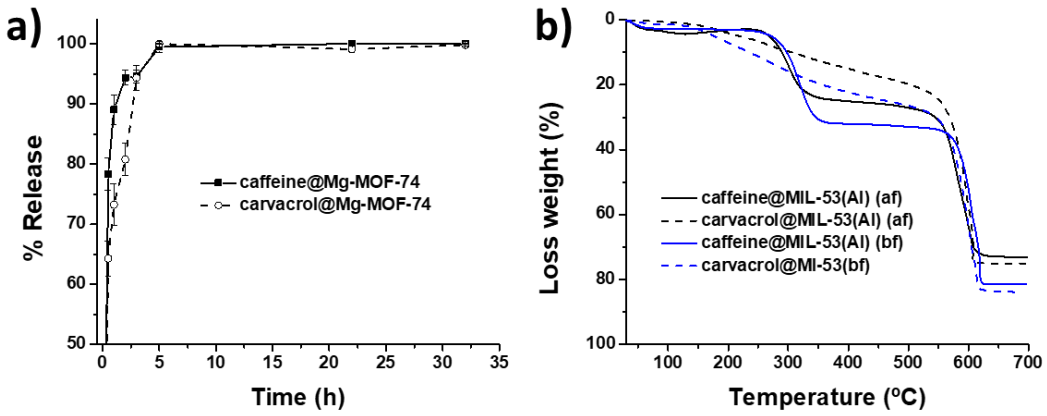


**Figure 8.** Release profiles at 25 °C for caffeine@Mg-MOF-74 and carvacrol@Mg-MOF-74 in distilled water (a) and TGA curves of the solids before (bf) and after (af) the release experiment, i.e. the remaining solids recovered by centrifugation from aqueous solution after 10 days in the release system, for caffeine@MIL-53(Al) and carvacrol@MIL-53(Al) (b).

## 4. CONCLUSIONS

The encapsulation of bioactive molecules caffeine and carvacrol in two different MOFs, the flexible MIL-53(Al) and the rigid Mg-MOF-74, has been demonstrated. In all cases, the loadings were higher under supercritical $CO_2$ conditions than applying the conventional liquid phase procedure in ethanol. In fact, the encapsulation in Mg-MOF-74 was only possible in the supercritical phase. The encapsulation was demonstrated using the measurements of XRD diffraction, TGA analysis and gas adsorption, while the Raman spectroscopy was useful to study the host-guest interactions. The encapsulation with sc-$CO_2$

showed clear advantages compared with the conventional technique: it required no later purification avoiding in this manner the steps of separation and drying in liquid phase, no ethanol contaminated the product and the excess of additive remained in the system as pure solid or liquid, therefore it could be reused easily. This methodology could be potentially applied to any soluble additive in sc-$CO_2$ and particularly to those sensitive to temperature or unstable in solution. Consequently, and after the displayed results, this is a promising procedure for encapsulation in MOFs.

## ASSOCIATED CONTENT

**Supporting Information**. MOFs initial characterization, $N_2$ and $CO_2$ isotherms, SEM image and Raman shifts. This material is available free of charge via the Internet at http://pubs.acs.org.

## AUTHOR INFORMATION

### Corresponding Author

* soraya.rodriguez@uva.es, coronas@unizar.es

## ACKNOWLEDGMENTS

The authors acknowledge financial support from the Aragón Government (DGA, T43-17R) and the European Social Fund. Íñigo Echániz is acknowledged for his help with Raman spectrometer use. Soraya Rodríguez Rojo acknowledges Junta de Castilla y León and FEDER 2014-2020 for her postdoctoral contract under Project VA040U16.

## REFERENCES

[1] J. Lee, O.K. Farha, J. Roberts, K. a Scheidt, S.T. Nguyen, J.T. Hupp, Metal-organic framework materials as catalysts., Chem. Soc. Rev. 38 (2009) 1450–1459. doi:10.1039/b807080f.

[2] J.-R. Li, R.J. Kuppler, H.-C. Zhou, Selective gas adsorption and separation in metal-organic frameworks., Chem. Soc. Rev. 38 (2009) 1477–1504. doi:10.1039/b802426j.

[3] S. Sorribas, P. Gorgojo, C. Téllez, J. Coronas, A.G. Livingston, High flux thin film nanocomposite membranes based on metal-organic frameworks for organic solvent nanofiltration, J. Am. Chem. Soc. 135 (2013) 15201–15208. doi:10.1021/ja407665w.

[4] P. Horcajada, C. Serre, G. Maurin, N.A. Ramsahye, F. Balas, M. Vallet-Regí, M. Sebban, F. Taulelle, G. Férey, Flexible Porous Metal-Organic Frameworks for a Controlled Drug Delivery, J. Am. Chem. Soc. 130 (2008) 6774–6780. doi:10.1021/ja710973k.

[5] L. Paseta, G. Potier, S. Abbott, J. Coronas, Using Hansen solubility parameters to study the

encapsulation of caffeine in MOFs, Org. Biomol. Chem. 13 (2015) 1724–1731. doi:10.1039/C4OB01898B.

[6] O.M. Yaghi, H. Li, M. Eddaoudi, M. O'Keeffe, Design and synthesis of an exceptionally stable and highly porous metal-organic framework, Nature. 402 (1999) 276–279. doi:10.1038/46248.

[7] T. Loiseau, C. Serre, C. Huguenard, G. Fink, F. Taulelle, M. Henry, T. Bataille, G. Férey, A rationale for the large breathing of the porous aluminum terephthalate (MIL-53) upon hydration., Chemistry. 10 (2004) 1373–1382. doi:10.1002/chem.200305413.

[8] C. Serre, C. Mellot-Draznieks, S. Surblé, N. Audebrand, Y. Filinchuk, G. Férey, Role of Solvent-Host Interactions That Lead to Very Large Swelling of Hybrid Frameworks, Science (80-. ). 315 (2007) 1828–1831. doi:10.1126/science.1137975.

[9] K.S. Park, Z. Ni, A.P. Cote, J.Y. Choi, R. Huang, F.J. Uribe-Romo, H.K. Chae, M. O'Keeffe, O.M. Yaghi, A.P. Côté, J.Y. Choi, R. Huang, F.J. Uribe-Romo, H.K. Chae, M. O'Keeffe, O.M. Yaghi, Exceptional chemical and thermal stability of zeolitic imidazolate frameworks., Proc. Natl. Acad. Sci. U. S. A. 103 (2006) 10186–91. doi:10.1073/pnas.0602439103.

[10] R.C. Huxford, J. Della Rocca, W. Lin, Metal-organic frameworks as potential drug carriers, Curr. Opin. Chem. Biol. (2010). doi:10.1016/j.cbpa.2009.12.012.

[11] D. Cunha, C. Gaudin, I. Colinet, P. Horcajada, G. Maurin, C. Serre, Rationalization of the entrapping of bioactive molecules into a series of functionalized porous zirconium terephthalate MOFs, J. Mater. Chem. B. (2013). doi:10.1039/c2tb00366j.

[12] H. Zheng, Y. Zhang, L. Liu, W. Wan, P. Guo, A.M. Nyström, X. Zou, One-pot Synthesis of Metal-Organic Frameworks with Encapsulated Target Molecules and Their Applications for Controlled Drug Delivery, J. Am. Chem. Soc. (2016). doi:10.1021/jacs.5b11720.

[13] S.R. Miller, D. Heurtaux, T. Baati, P. Horcajada, J.M. Grenèche, C. Serre, Biodegradable therapeutic MOFs for the delivery of bioactive molecules, Chem. Commun. (2010). doi:10.1039/c001181a.

[14] L.E. Kreno, K. Leong, O.K. Farha, M. Allendorf, R.P. Van Duyne, J.T. Hupp, Metal-organic framework materials as chemical sensors, Chem. Rev. (2012). doi:10.1021/cr200324t.

[15] J. Della Rocca, D. Liu, W. Lin, Nanoscale Metal-Organic Frameworks for Biomedical Imaging and Drug Delivery, Acc. Chem. Res. (2011). doi:10.1021/ar200028a.

[16] L. Paseta, E. Simón-Gaudó, F. Gracia-Gorría, J. Coronas, Encapsulation of essential oils in porous silica and MOFs for trichloroisocyanuric acid tablets used for water treatment in swimming pools, Chem. Eng. J. 292 (2016) 28–34. doi:10.1016/j.cej.2016.02.001.

[17] P. Horcajada, T. Chalati, C. Serre, B. Gillet, C. Sebrie, T. Baati, J.F. Eubank, D. Heurtaux, P.

Clayette, C. Kreuz, J.-S. Chang, Y.K. Hwang, V. Marsaud, P.-N. Bories, L. Cynober, S. Gil, G. Férey, P. Couvreur, R. Gref, Porous metal-organic-framework nanoscale carriers as a potential platform for drug delivery and imaging., Nat. Mater. 9 (2010) 172–178. doi:10.1038/nmat2608.

[18] D. Cunha, M. Ben Yahia, S. Hall, S.R. Miller, H. Chevreau, E. Elkaïm, G. Maurin, P. Horcajada, C. Serre, Rationale of drug encapsulation and release from biocompatible porous metal-organic frameworks, Chem. Mater. 25 (2013) 2767–2776. doi:10.1021/cm400798p.

[19] N. Liédana, P. Lozano, A. Galve, C. Tellez, J. Coronas, The template role of caffeine in its one-step encapsulation in MOF NH2-MIL-88B(Fe), J. Mater. Chem. B. 2 (2014) 1144–1151. doi:10.1039/C3TB21707H.

[20] S. Hermes, M.-K. Schröter, R. Schmid, L. Khodeir, M. Muhler, A. Tissler, R.W. Fischer, R. a Fischer, Metal@MOF: loading of highly porous coordination polymers host lattices by metal organic chemical vapor deposition., Angew. Chem. Int. Ed. Engl. 44 (2005) 6237–41. doi:10.1002/anie.200462515.

[21] O.K. Farha, J.T. Hupp, Rational design, synthesis, purification, and activation of metal-organic framework materials, Acc. Chem. Res. 43 (2010) 1166–1175. doi:10.1021/ar1000617.

[22] J.E. Mondloch, O. Karagiaridi, O.K. Farha, J.T. Hupp, Activation of metal–organic framework materials, CrystEngComm. 15 (2013) 9258. doi:10.1039/c3ce41232f.

[23] A.P. Nelson, O.K. Farha, K.L. Mulfort, J.T. Hupp, Supercritical Processing as a Route to High Internal Surface Areas and Permanent Microporosity in Metal Organic Framework Materials, J. Am. Chem. Soc. 131 (2009) 458–460. doi:doi:10.1021/ja808853q.

[24] O.K. Farha, I. Eryazici, N.C. Jeong, B.G. Hauser, C.E. Wilmer, A.A. Sarjeant, R.Q. Snurr, S.T. Nguyen, A.Ö. Yazaydin, J.T. Hupp, Metal-organic framework materials with ultrahigh surface areas: Is the sky the limit?, J. Am. Chem. Soc. 134 (2012) 15016–15021. doi:10.1021/ja3055639.

[25] M.J. Cocero, Á. Martín, F. Mattea, S. Varona, Encapsulation and co-precipitation processes with supercritical fluids: Fundamentals and applications, J. Supercrit. Fluids. 47 (2009) 546–555. doi:10.1016/j.supflu.2008.08.015.

[26] M.P. Fernández-Ronco, J. Kluge, J. Krieg, S. Rodríguez-Rojo, B. Andreatta, R. Luginbuehl, M. Mazzotti, J. Sague, Improving the wear resistance of UHMWPE implants by in situ precipitation of hyaluronic acid using supercritical fluid technology, J. Supercrit. Fluids. 95 (2014) 204–213. doi:10.1016/j.supflu.2014.08.031.

[27] A.P. Almeida, S. Rodríguez-Rojo, A.T. Serra, H. Vila-Real, A.L. Simplicio, I. Delgadilho, S. Beirão Da Costa, L. Beirão Da Costa, I.D. Nogueira, C.M.M. Duarte, Microencapsulation of oregano essential oil in starch-based materials using supercritical fluid technology, Innov. Food

Sci. Emerg. Technol. 20 (2013) 140–145. doi:10.1016/j.ifset.2013.07.009.

[28] M. Salgado, F. Santos, S. Rodríguez-Rojo, R.L. Reis, A.R.C. Duarte, M.J. Cocero, Development of barley and yeast β-glucan aerogels for drug delivery by supercritical fluids, J. CO2 Util. 22 (2017) 262–269. doi:10.1016/j.jcou.2017.10.006.

[29] K. Matsuyama, N. Hayashi, M. Yokomizo, T. Kato, K. Ohara, T. Okuyama, Supercritical carbon dioxide-assisted drug loading and release from biocompatible porous metal–organic frameworks, J. Mater. Chem. B. 2 (2014) 7551–7558. doi:10.1039/C4TB00725E.

[30] A.M. López-Periago, J. Fraile, C.A. García-González, C. Domingo, Impregnation of a triphenylpyrylium cation into zeolite cavities using supercritical CO2, J. Supercrit. Fluids. 50 (2009) 305–312. doi:10.1016/j.supflu.2009.06.016.

[31] K. Leicht, G. Hartigan, R. D´Orazio, CO2 recovery process for supercritical extraction US6960242B2, 2003.

[32] K.P. Johnston, J.M. Dobbs, J.M. Wong, Nonpolar Co-Solvents for Solubility Enhancement in Supercritical Fluid Carbon Dioxide, J. Chem. Eng. Data. 31 (1986) 303–308. doi:10.1021/je00045a014.

[33] P.D.C. Dietzel, R. Blom, H. Fjellvåg, Base-induced formation of two magnesium metal-organic framework compounds with a bifunctional tetratopic ligand, Eur. J. Inorg. Chem. (2008) 3624–3632. doi:10.1002/ejic.200701284.

[34] J.B. DeCoste, G.W. Peterson, B.J. Schindler, K.L. Killops, M. a. Browe, J.J. Mahle, The effect of water adsorption on the structure of the carboxylate containing metal–organic frameworks Cu-BTC, Mg-MOF-74, and UiO-66, J. Mater. Chem. A. 1 (2013) 11922. doi:10.1039/c3ta12497e.

[35] J. Heller, Biodegradable polymers in controlled drug delivery., Crit. Rev. Ther. Drug Carrier Syst. 1 (1984) 39–90.

[36] A. Kumari, S.K. Yadav, S.C. Yadav, Biodegradable polymeric nanoparticles based drug delivery systems, Colloids Surfaces B Biointerfaces. 75 (2010) 1–18. doi:10.1016/j.colsurfb.2009.09.001.

[37] S.R. Miller, D. Heurtaux, T. Baati, P. Horcajada, J.-M. Grenèche, C. Serre, Biodegradable therapeutic MOFs for the delivery of bioactive molecules, Chem. Commun. 46 (2010) 4526. doi:10.1039/c001181a.

[38] W. Cai, C.C. Chu, G. Liu, Y.X.J. Wáng, Metal-Organic Framework-Based Nanomedicine Platforms for Drug Delivery and Molecular Imaging, Small. 11 (2015) 4806–4822. doi:10.1002/smll.201500802.

[39] U. Kopcak, R.S. Mohamed, Caffeine solubility in supercritical carbon dioxide/co-solvent mixtures, J. Supercrit. Fluids. 34 (2005) 209–214. doi:10.1016/j.supflu.2004.11.016.

[40] G.I. Burgos-Solórzano, J.F. Brennecke, M.A. Stadtherr, Solubility measurements and modeling of molecules of biological and pharmaceutical interest with supercritical CO2, Fluid Phase Equilib. 220 (2004) 57–69. doi:10.1016/j.fluid.2004.01.036.

[41] E. Lack, H. Seidlitz, Commercial scale decaffeination of coffee and tea using supercritical CO2 BT - Extraction of Natural Products Using Near-Critical Solvents, in: M.B. King, T.R. Bott (Eds.), Springer Netherlands, Dordrecht, 1993: pp. 101–139. doi:10.1007/978-94-011-2138-5_5.

[42] S. Devautour-Vinot, C. Martineau, S. Diaby, M. Ben-Yahia, S. Miller, C. Serre, P. Horcajada, D. Cunha, F. Taulelle, G. Maurin, Caffeine confinement into a series of functionalized porous zirconium MOFs: A joint experimental/modeling exploration, J. Phys. Chem. C. 117 (2013) 11694–11704. doi:10.1021/jp402916y.

[43] N. Liédana, E. Marín, C. Téllez, J. Coronas, One-step encapsulation of caffeine in SBA-15 type and non-ordered silicas, Chem. Eng. J. 223 (2013) 714–721. doi:10.1016/j.cej.2013.03.041.

[44] C. Labay, J.M. Canal, A. Navarro, C. Canal, Corona plasma modification of polyamide 66 for the design of textile delivery systems for Cosmetic therapy, Appl. Surf. Sci. (2014). doi:10.1016/j.apsusc.2014.07.191.

[45] L. Rubio, C. Alonso, L. Coderch, J.L. Parra, M. Martí, J. Cebrián, J.A. Navarro, M. Lis, J. Valldeperas, Skin Delivery of Caffeine Contained in Biofunctional Textiles, Text. Res. J. (2010). doi:10.1177/0040517509358798.

[46] G.H. Kamimori, C.S. Karyekar, R. Otterstetter, D.S. Cox, T.J. Balkin, G.L. Belenky, N.D. Eddington, The rate of absorption and relative bioavailability of caffeine administered in chewing gum versus capsules to normal healthy volunteers, Int. J. Pharm. (2002). doi:10.1016/S0378-5173(01)00958-9.

[47] G.A. Leeke, R. Santos, M.B. King, Vapor-liquid equilibria for the carbon dioxide + carvacrol system at elevated pressures, J. Chem. Eng. Data. 46 (2001) 541–545. doi:10.1021/je000342k.

[48] R.J.W. Lambert, P.N. Skandamis, P.J. Coote, G.J.E. Nychas, A study of the minimum inhibitory concentration and mode of action of oregano essential oil, thymol and carvacrol, J. Appl. Microbiol. 91 (2001) 453–462. doi:10.1046/j.1365-2672.2001.01428.x.

[49] A. Nostro, T. Papalia, Antimicrobial Activity of Carvacrol: Current Progress and Future Prospectives, Recent Pat. Antiinfect. Drug Discov. 7 (2012) 28–35. doi:10.2174/157489112799829684.

[50] R. Baranauskiene, P.R. Venskutonis, K. Dewettinck, R. Verhé, Properties of oregano (Origanum vulgare L.), citronella (Cymbopogon nardus G.) and marjoram (Majorana hortensis L.) flavors encapsulated into milk protein-based matrices, Food Res. Int. 39 (2006) 413–425.

doi:10.1016/j.foodres.2005.09.005.

[51] L. Keawchaoon, R. Yoksan, Preparation, characterization and in vitro release study of carvacrol-loaded chitosan nanoparticles, Colloids Surfaces B Biointerfaces. 84 (2011) 163–171. doi:10.1016/j.colsurfb.2010.12.031.

[52] M. Ramos, A. Beltrán, M. Peltzer, A.J.M. Valente, M. del C. Garrigós, Release and antioxidant activity of carvacrol and thymol from polypropylene active packaging films, LWT - Food Sci. Technol. 58 (2014) 470–477. doi:10.1016/j.lwt.2014.04.019.

[53] A. Iannitelli, R. Grande, A. di Stefano, M. di Giulio, P. Sozio, L.J. Bessa, S. Laserra, C. Paolini, F. Protasi, L. Cellini, Potential antibacterial activity of carvacrol-loaded poly(DL-lactide-co-glycolide) (PLGA) nanoparticles against microbial biofilm, Int. J. Mol. Sci. 12 (2011) 5039–5051. doi:10.3390/ijms12085039.

[54] J.E.D. Davies, Vibrational spectroscopic studies of host-guest compounds, ARI - An Int. J. Phys. Eng. Sci. 51 (1998) 120–125. doi:10.1007/s007770050043.

[55] Y. Huang, J.H. Leech, E.A. Havenga, R.R. Poissant, Investigations of host-guest interactions in zeolitic systems by FT-Raman spectroscopy, Microporous Mesoporous Mater. 48 (2001) 95–102. doi:10.1016/S1387-1811(01)00363-8.

[56] S.G. Kazarian, G.G. Martirosyan, Spectroscopy of polymer/drug formulations processed with supercritical fluids: in situ ATR–IR and Raman study of impregnation of ibuprofen into PVP, Int. J. Pharm. 232 (2002) 81–90. doi:https://doi.org/10.1016/S0378-5173(01)00905-X.

[57] D.Y. Siberio-Pérez, A.G. Wong-Foy, O.M. Yaghi, A.J. Matzger, Raman Spectroscopic Investigation of CH4 and N2 Adsorption in Metal-Organic Frameworks, Chem. Mater. 19 (2007) 3681–3685. doi:10.1021/cm070542g.

[58] A. Bamberger, G. Sieder, G. Maurer, High-pressure (vapor+liquid) equilibrium in binary mixtures of (carbon dioxide+water or acetic acid) at temperatures from 313 to 353 K, J. Supercrit. Fluids. 17 (2000) 97–110. doi:https://doi.org/10.1016/S0896-8446(99)00054-6.

[59] A.N. Sabirzyanov, A.P. Il'in, A.R. Akhunov, F.M. Gumerov, Solubility of Water in Supercritical Carbon Dioxide, High Temp. 40 (2002) 203–206. doi:10.1023/A:1015294905132.

[60] D. Britt, H. Furukawa, B. Wang, T.G. Glover, O.M. Yaghi, Highly efficient separation of carbon dioxide by a metal-organic framework replete with open metal sites., Proc. Natl. Acad. Sci. U. S. A. 106 (2009) 20637–20640. doi:10.1073/pnas.0909718106.

[61] N. Liédana, A. Galve, C. Rubio, C. Téllez, J. Coronas, CAF@ZIF-8: One-step encapsulation of caffeine in MOF, ACS Appl. Mater. Interfaces. 4 (2012) 5016–5021. doi:10.1021/am301365h.

[62] J. Maultzsch, H. Telg, S. Reich, C. Thomsen, Radial breathing mode of single-walled carbon

nanotubes: Optical transition energies and chiral-index assignment, Phys. Rev. B - Condens. Matter Mater. Phys. 72 (2005) 205438. doi:10.1103/PhysRevB.72.205438.

[63] S. Zuluaga, E.M.A. Fuentes-Fernandez, K. Tan, F. Xu, J. Li, Y.J. Chabal, T. Thonhauser, Understanding and controlling water stability of MOF-74, J. Mater. Chem. A. 4 (2016) 5176–5183. doi:10.1039/c5ta10416e.